

# The refocused INADEQUATE MAS NMR experiment in multiple spin-systems: Interpreting observed correlation peaks and optimising lineshapes

Sylvian Cadars<sup>a,1</sup>, Julien Sein<sup>a</sup>, Luminita Duma<sup>a,2</sup>, Anne Lesage<sup>a</sup>, Tran N. Pham<sup>b,3</sup>, Jay H. Baltisberger<sup>c</sup>, Steven P. Brown<sup>b</sup>, Lyndon Emsley<sup>a,\*</sup>

<sup>a</sup> Laboratoire de Chimie (UMR 5182 CNRS/ENS Lyon), École Normale Supérieure de Lyon, 46 allée d'Italie, 69364 Lyon Cedex 07, France

<sup>b</sup> Department of Physics, University of Warwick, Coventry CV4 7AL, UK

<sup>c</sup> Department of Chemistry, Berea College, Berea, KY 40404, USA

Received 3 April 2007

Available online 6 June 2007

## Abstract

The robustness of the refocused INADEQUATE MAS NMR pulse sequence for probing through-bond connectivities has been demonstrated in a large range of solid-state applications. This pulse sequence nevertheless suffers from artifacts when applied to multispin systems, *e.g.* uniformly labeled <sup>13</sup>C solids, which distort the lineshapes and can potentially result in misleading correlation peaks. In this paper, we present a detailed account that combines product-operator analysis, numerical simulations and experiments of the behavior of a three-spin system during the refocused INADEQUATE pulse sequence. The origin of undesired anti-phase contributions to the spectral lineshapes are described, and we show that they do not interfere with the observation of long-range correlations (*e.g.* two-bond <sup>13</sup>C–<sup>13</sup>C correlations). The suppression of undesired contributions to the refocused INADEQUATE spectra is shown to require the removal of zero-quantum coherences within a *z*-filter. A method is proposed to eliminate zero-quantum coherences through dephasing by heteronuclear dipolar couplings, which leads to pure in-phase spectra.

© 2007 Elsevier Inc. All rights reserved.

**Keywords:** Solid-state NMR; Zero-quantum coherences; *z*-filter; Multispin systems; INADEQUATE; Solid-state; Magic angle spinning; Scalar coupling; Through-bond spectroscopy

## 1. Introduction

Through-bond mediated homonuclear experiments, which have been one of the cornerstones of solution-state NMR for several decades have recently been increasingly utilized in solid-state NMR. Their advantage is to provide the unambiguous identification of through-bond chemical con-

nectivities, as compared to dipolar-coupling mediated experiments that cannot distinguish between bonding and non-bonding through-space proximities. They rely on the use of the isotropic scalar (*J*) coupling interaction which is generally weak as compared to dipolar couplings. Two distinct classes of *J*-coupling mediated experiments have been introduced. On the one hand, symmetry-based pulse sequences, such as the total through-bond spectroscopy (TOBSY)<sup>4</sup>

\* Corresponding author. Fax : +33 4 72 72 88 60.

E-mail address: [lyndon.emsley@ens-lyon.fr](mailto:lyndon.emsley@ens-lyon.fr) (L. Emsley).

<sup>1</sup> Present address: Department of Chemical Engineering, University of California, Santa Barbara, CA 93106, USA.

<sup>2</sup> Present address: Département de Chimie, École Normale Supérieure, associé au CNRS, 24 rue Lhomond, 75231 Paris Cedex 05, France.

<sup>3</sup> Present address: Chemical Development, Analytical Sciences, Glaxo-SmithKline PLC, Gunnels Wood Road, Stevenage, SG1 2NY, UK.

<sup>4</sup> Abbreviations: TOBSY, total through-bond spectroscopy; INADEQUATE, incredible natural abundance double quantum transfer experiment; CR, composite refocusing; UC2QF COSY, uniform-sign cross-peak double quantum filtered correlation spectroscopy; TQ, triple-quantum; DD, dipole–dipole; CSA, chemical shift anisotropy, DQ, double quantum; ZQ, zero-quantum; CP, cross polarization; PDS, proton-driven spin diffusion.

experiment, use the spin-space symmetry properties of the different interactions to remove the undesired chemical shift anisotropy (CSA) and dipolar interactions, thus leaving only the homonuclear  $J$ -couplings [1–5]. Although these are rather complicated pulse sequences, most of which require the use of specific magic angle spinning (MAS) frequencies, they have been widely applied to enriched multi-spin systems. On the other hand, other methods have been adapted from solution NMR, which use coherence-transfer echoes [6] to transfer the magnetization between scalar-coupled nuclei. In addition to their simplicity they have the great advantage of allowing the connectivity patterns along a given spin system to be traced out (as opposed to TOBSY-type spectra where all the sites of a given spin system appear correlated to each other, i.e. in a linear  $A$ – $B$ – $C$  spin system with  $J_{AC} = 0$  Hz,  $A$  and  $C$  would appear correlated). These include the solid-state INADEQUATE [7,8] and INADEQUATE-CR [9], the refocused INADEQUATE [10], the UC2QF-COSY [11–13], spin-state selective experiments [14], and the recently introduced  $J$ -mediated triple-quantum (TQ) experiment [15]. In this paper, we focus on the refocused INADEQUATE experiment, whose robustness has been repeatedly demonstrated in a wide range of  $^{13}\text{C}$ -enriched [16–20] or  $^{15}\text{N}$ -enriched [21,22] and  $^{13}\text{C}$  natural abundance [23–28] polycrystalline organic systems, as well as in disordered [29–31] organic systems and in crystalline and disordered inorganic solids [32–36].

Despite its success, the refocused INADEQUATE experiment may suffer from some artifacts in certain cases. In particular, it has been shown that peaks corresponding to through-space connectivities can appear at or close to rotational resonance conditions, in particular for the  $n = 0$  rotational resonance (i.e. two sites having the same isotropic chemical shift), in the case where two nuclei with a non-vanishing through-space DD coupling have CSA tensors with different principal values or orientations [35].

This paper considers the lineshape distortions and unexpected correlation peaks that are observed when the refocused INADEQUATE experiment is applied to samples which consist of spin systems that extend beyond simple spin pairs, as is the case in high abundance ( $^{31}\text{P}$ ) or isotopically enriched ( $^{13}\text{C}$ ,  $^{15}\text{N}$ ) systems, with a consideration here of the specific case of uniformly  $^{13}\text{C}$ -labeled polycrystalline L-alanine. A detailed analysis using the standard product-operator approach commonly employed for solution-state experiments is presented, whose validity is discussed by means of comparison with experiments and numerical simulations. The improvements achieved by the addition of a  $z$ -filter are discussed; in particular, it is shown that the crucial issue to tackle is the removal of contributions due to zero-quantum (ZQ) coherences. Strategies for removing such ZQ coherences by means of solution-state-NMR based approaches, as well as methods utilizing specific solid-state interactions, are considered.

## 2. Nature and origin of the undesired contributions

The pulse sequence for the refocused INADEQUATE experiment using cross polarization to create the initial transverse magnetization is shown in Fig. 1(a), together with the corresponding  $X$  (e.g.,  $^{13}\text{C}$ ) nucleus coherence-transfer pathway [37] to be selected using phase cycling. The pulse sequence can be explained using a product-operator [38] description of the density matrix evolution on a system of two  $J$ -coupled spins  $A$  and  $B$ . Of course, such a solution-state-based analysis is only valid in a limited number of regimes where the effect of solid-state anisotropic interactions can be neglected: namely, in the case that all rotational resonance conditions are avoided, and the spinning frequency is sufficiently large that the homonuclear dipolar couplings between the detected nuclei and CSA interactions are completely averaged out over an integral number of rotor periods. Moreover, the strong heteronuclear dipolar couplings to the dense network of protons are assumed to be entirely removed by efficient heteronuclear decoupling. Furthermore, the product-operator formalism assumes, first, ideal (infinitely short) pulses and, second, homonuclear  $J$ -couplings that are small as compared to the isotropic chemical shift differences [38].

After cross polarization (CP) from protons to the  $X$  spins, we consider the initial density matrix  $\sigma(0) = -M_A^0 A_y - M_B^0 B_y$ , where  $M_A^0$  and  $M_B^0$  correspond to the magnitude of the transverse magnetization created by CP on spins  $A$  and  $B$ , respectively. A first  $\tau$ – $\pi$ – $\tau$  spin echo generates anti-phase coherences through  $J$ -coupling evolution, with best theoretical efficiency for a spin-echo delay  $\tau = 1/(4J_{AB})$ , ignoring transverse dephasing.

$$\sigma(0) \xrightarrow{\tau-\pi-\tau} M_A^0 (A_y c_{AB} + 2A_x B_z s_{AB}) + M_B^0 (B_y c_{AB} + 2A_z B_x s_{AB}) \quad (1)$$

where  $c_{AB} = \cos(2\pi J_{AB}\tau)$  and  $s_{AB} = \sin(2\pi J_{AB}\tau)$ . The anti-phase coherences are then converted to a mixture of double-quantum (DQ) and zero-quantum (ZQ) coherences between  $J$ -coupled nuclei by the first  $90^\circ$  pulse.

$$\xrightarrow{(\pi/2)_x} M_A^0 (A_z c_{AB} - 2A_x B_y s_{AB}) + M_B^0 (B_z c_{AB} - 2A_y B_x s_{AB}) \quad (2)$$

Terms of coherence order 0 in  $t_1$  are removed by appropriate phase cycling of the first  $90^\circ$  and the first  $180^\circ$  pulse to select DQ coherence, which yields a loss in overall efficiency of 50%.<sup>5</sup>

$$\xrightarrow{\text{DQselection}} -\frac{M_A^0}{2} s_{AB} (2A_x B_y + 2A_y B_x) - \frac{M_B^0}{2} s_{AB} (2A_y B_x + 2A_x B_y) \quad (3)$$

<sup>5</sup> Terms of the form  $2A_x B_y$  are first expressed as combinations of  $A^+$ ,  $A^-$ ,  $B^+$ , and  $B^-$ . Then contributions of coherence order 0 ( $A^+ B^-$ ,  $A^- B^+$ ) are removed while those of coherence order 2 ( $A^+ B^+$ ,  $A^- B^-$ ) remain. Finally, the remaining terms are expressed again as combinations of  $A_x$ ,  $A_y$ ,  $B_x$  and  $B_y$ .

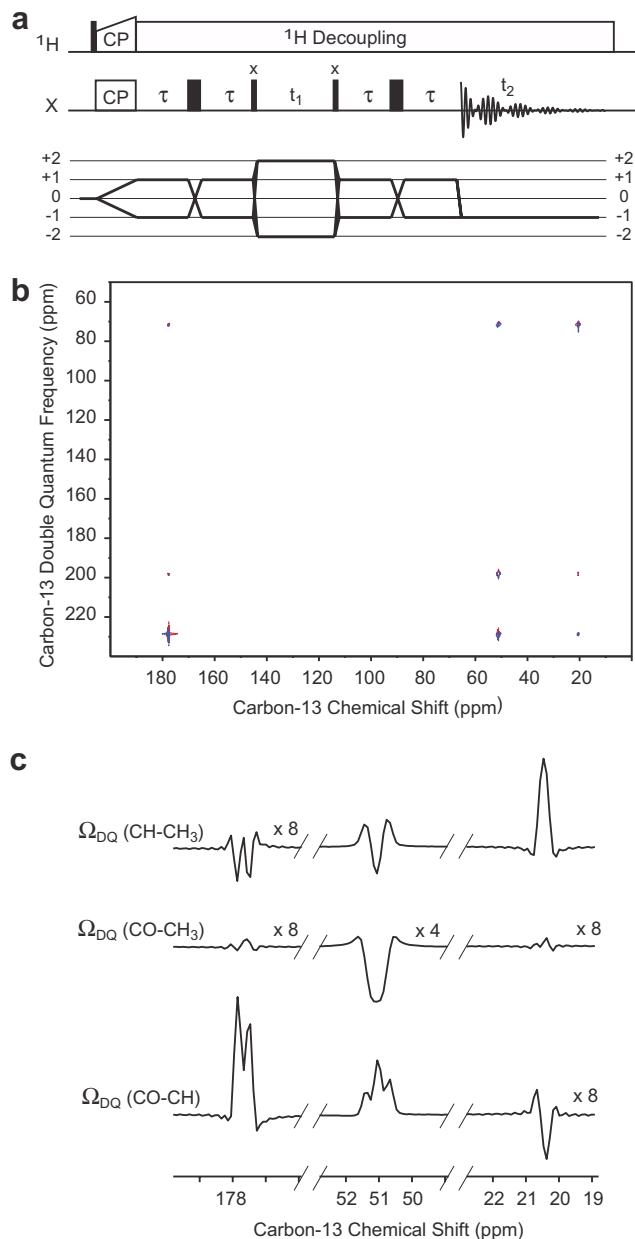


Fig. 1. (a) Pulse sequence and coherence-transfer pathway diagram [37] of the refocused INADEQUATE experiment, which provides homonuclear through-bond correlation spectra in solids, as proposed by Lesage and co-workers [10]. (b)  $^{13}\text{C}$  refocused INADEQUATE 2D spectrum of fully  $^{13}\text{C}$ -enriched L-alanine, obtained with the pulse sequence shown in (a). Contour levels correspond to  $\pm 1$ ,  $\pm 21$ ,  $\pm 41$ ,  $\pm 61$  and  $\pm 81\%$  of the maximum intensity, positive contours being indicated in blue and negative contours in red. (c) Traces extracted from the 2D refocused INADEQUATE spectrum shown in (b). The rows, from top to bottom, respectively, correspond to the double-quantum frequency of the CH-CH<sub>3</sub>, CO-CH<sub>3</sub> and CO-CH correlations, while the columns correspond to the CO, CH and CH<sub>3</sub> resonances in  $F_2$ , respectively. The experiment was carried out at 125.8 MHz  $^{13}\text{C}$  Larmor frequency, spinning at 25 kHz, using a  $\tau$  delay of 3 ms. No apodization was applied in the direct  $F_2$  dimension. The vertical scaling, if any, applied to a given subspectrum is indicated on the figure.

The remaining DQ coherences evolve under the sum of the chemical shifts  $\Omega_{AB} = \omega_A + \omega_B$  during the indirect period, and are then converted back to anti-phase coherences.

Only contributions obtained for  $t_1 = 0$  are considered here for simplicity:

$$\xrightarrow{(\pi/2)_x} -\frac{M_A^0}{2} s_{AB}(2A_x B_z + 2A_z B_x) - \frac{M_B^0}{2} s_{AB}(2A_z B_x + 2A_x B_z) \quad (4)$$

The second spin echo achieves the transformation of the anti-phase coherences (complete only for  $\tau = 1/(4J_{AB})$ ) into in-phase coherence for detection:

$$\xrightarrow{\tau - \pi_x - \tau} \frac{M_A^0}{2} (2A_x B_z s_{AB} c_{AB} + A_y s_{AB}^2 + 2A_z B_x s_{AB} c_{AB} + B_y s_{AB}^2) + \frac{M_B^0}{2} (2A_x B_z s_{AB} c_{AB} + A_y s_{AB}^2 + 2A_z B_x s_{AB} c_{AB} + B_y s_{AB}^2) \quad (5)$$

For  $\tau = 1/(4J_{AB})$ ,  $c_{AB} = 0$  and  $s_{AB} = 1$ , and the anti-phase contributions vanish.

$$\sigma(t_2 = 0) = \frac{M_A^0}{2} (A_y + B_y) + \frac{M_B^0}{2} (A_y + B_y) \quad (6)$$

When applied to an isolated  $J$ -coupled spin pair, the refocused INADEQUATE experiment (for  $\tau = 1/(4J_{AB})$ ) thus yields a pair of in-phase correlation peaks at the same DQ frequency ( $\Omega_{AB} = \omega_A + \omega_B$ ) in the indirect dimension, at the sum of their individual frequencies.

We now turn our attention to three-spin systems. Fig. 1(b) shows the contour plot of a refocused INADEQUATE spectrum recorded for 99%  $^{13}\text{C}$ -enriched L-alanine. At first sight we see that, as expected, the major features are intense peaks observed at  $(\Omega_{\text{DQ}}(\text{CH}-\text{CH}_3), \omega(\text{CH}))$ ,  $(\Omega_{\text{DQ}}(\text{CH}-\text{CH}_3), \omega(\text{CH}_3))$ ,  $(\Omega_{\text{DQ}}(\text{CO}-\text{CH}), \omega(\text{CO}))$ , and  $(\Omega_{\text{DQ}}(\text{CO}-\text{CH}), \omega(\text{CH}))$ , that correspond to the expected cross peaks for the one-bond connectivities in this system. Upon close inspection, it is, however, evident that these peaks exhibit marked lineshape distortions, being not purely in-phase, as illustrated in Fig. 1(c) by the traces extracted at three DQ frequencies corresponding to the CH-CH<sub>3</sub> (72 ppm, top), the CO-CH<sub>3</sub> (199 ppm, middle) and CO-CH (228 ppm, bottom) pairs. Moreover, an intense negative peak is observed at  $(\Omega_{\text{DQ}}(\text{CO}-\text{CH}_3), \omega(\text{CH}))$ ; as discussed further below, this is an example of a so-called “relayed peak” between two non-bonded nuclei that share a common coupling partner [39], whose appearance has been noted by Titman and co-workers in a  $^{13}\text{C}$  refocused INADEQUATE spectrum of 50%  $^{13}\text{C}$ -enriched CsC<sub>60</sub> (see Fig. 5 of Ref. [16]). Finally, non-negligible though weak peaks which appear to be largely anti-phase are also observed at other positions in the spectrum; in particular at  $(\Omega_{\text{DQ}}(\text{CO}-\text{CH}_3), \omega(\text{CO}))$  and  $(\Omega_{\text{DQ}}(\text{CO}-\text{CH}_3), \omega(\text{CH}_3))$ , corresponding to the expected positions of long-range correlations between CO and CH<sub>3</sub> through the associated two-bond  $J$ -coupling. An important issue is to determine whether these peaks are due to such a small long-range  $^{13}\text{CO}-^{13}\text{CH}_3$  coupling or arise from undesired contributions to the spectrum, in which case they could lead to erroneous interpretation.

In order to determine the different possible contributions to the refocused INADEQUATE spectrum, a complete product-operator calculation of the density matrix evolution during the pulse sequence has been carried out on a three-spin system. Again, this approach is only valid for the conditions described above. In the following, a system of three-spins-1/2  $A$ ,  $B$ ,  $C$  will be considered, which can either be treated as a weakly-coupled linear system, with  $J_{AB} \neq 0$  Hz,  $J_{BC} \neq 0$  Hz and  $J_{AC} = 0$  Hz, or as a weakly-coupled triangular system having a non-zero  $J_{AC}$  coupling constant. The notation used here is different from the one commonly used in liquid-state NMR, where  $A$ ,  $B$  and  $C$  would refer to strongly-coupled spins, and where  $A$ ,  $M$  and  $X$  would be used instead to refer to a system of weakly-coupled spins. As was the case above for two coupled spins, the letter  $M^0$  designates the magnetization (here created after CP).

Table 1 lists the terms expected (in regimes fulfilling the conditions stated above) at the beginning of the direct detection period for the first point of the 2D refocused INADEQUATE spectrum, *i.e.* at  $t_2 = 0$  for  $t_1 = 0$ . They were obtained by applying the following sequence to the reduced initial density matrix  $\sigma_0^A = -M_A^0 A_y$ , where  $M_A^0$  corresponds to the magnitude of the transverse magnetization created by CP:

$$\tau - \pi_x - \tau - (\pi/2)_x - t_1 - (\pi/2)_x - \tau - \pi_x - \tau \quad (7)$$

Table 1

List of contributions to the refocused INADEQUATE, at  $t_2 = 0$  for  $t_1 = 0$ , arising from the simplified density matrix  $\sigma_0 = -M_A^0 A_y$ , in a triangular spin system ( $J_{AC} \neq 0$ )

Term	Build-up function	$F_1$ frequency	$F_2$ frequency
$A_y M_A^0 / 2$	$s_{AB}^2 c_{AC}^2$	$\Omega_{AB}$	$\omega_A$
	$\times c_{AB}^2 s_{AC}^2$	$\Omega_{AC}$	
	$\times -s_{AB}^2 s_{AC}^2$	$\Omega_{BC}$	
$B_y M_A^0 / 2$	$s_{AB}^2 c_{AC} c_{BC}$	$\Omega_{AB}$	$\omega_B$
$C_y M_A^0 / 2$	$\times c_{AB} s_{AC}^2 c_{BC}$	$\Omega_{AC}$	$\omega_C$
$2A_x B_z M_A^0 / 2$	$s_{AB} c_{AB} c_{AC}^2$	$\Omega_{AB}$	$\omega_A$
	$\times -s_{AB} c_{AB} s_{AC}^2$	$\Omega_{AC}$	
	$\times -s_{AB} c_{AB} s_{AC}^2$	$\Omega_{BC}$	
$2A_x C_z M_A^0 / 2$	$\times -s_{AB}^2 s_{AC} c_{AC}$	$\Omega_{AB}$	$\omega_A$
	$\times c_{AB}^2 s_{AC} c_{AC}$	$\Omega_{AC}$	
	$\times -s_{AB}^2 s_{AC} c_{AC}$	$\Omega_{BC}$	
$2A_z B_x M_A^0 / 2$	$s_{AB} c_{AB} c_{AC} c_{BC}$	$\Omega_{AB}$	$\omega_B$
$2B_x C_z M_A^0 / 2$	$-s_{AB}^2 c_{AC} s_{BC}$	$\Omega_{AB}$	
$2A_z C_x M_A^0 / 2$	$\times c_{AB} s_{AC} c_{AC} c_{BC}$	$\Omega_{AC}$	$\omega_C$
$2B_z C_x M_A^0 / 2$	$\times -c_{AB} s_{AC}^2 s_{BC}$	$\Omega_{AC}$	
$4A_y B_z C_z M_A^0 / 2$	$\times c_{AB} s_{AB} c_{AC} s_{AC}$	$\Omega_{AB}$	$\omega_A$
	$\times \Omega_{AC}$		
	$\times \Omega_{BC}$		
$4A_z B_y C_z M_A^0 / 2$	$c_{AB} s_{AB} c_{AC} s_{BC}$	$\Omega_{AB}$	$\omega_B$
$4A_z B_z C_y M_A^0 / 2$	$\times c_{AB} c_{AC} s_{AC} s_{BC}$	$\Omega_{AC}$	$\omega_C$

$\times$  indicates terms that would vanish for a linear spin system ( $J_{AC} = 0$  Hz).  $s_{KL}$  and  $c_{KL}$  are, respectively, equal to  $\sin(2\pi J_{KL}\tau)$  and  $\cos(2\pi J_{KL}\tau)$ .  $M_A^0$  represents the initial magnetization (after CP) on  $A$ .

where  $t_1 = 0$ , and zero-quantum coherences are discarded during  $t_1$ . The contributions listed in Table 1 thus correspond to only a third of the terms expected for a triangular spin system, and a complete list of terms can be obtained by the cyclic permutations  $A \rightarrow B \rightarrow C \rightarrow A$  and  $A \rightarrow C \rightarrow B \rightarrow A$  to give the terms corresponding to a reduced initial density matrix  $\sigma_0^B = -M_B^0 B_y$  and  $\sigma_0^C = -M_C^0 C_y$ , respectively. For a triangular spin system, the build-up functions of these terms as a function of  $\tau$  are somewhat complicated, as they may depend on the three distinct  $J$ -couplings, as shown in the table. The corresponding frequencies in the direct and indirect dimension of these terms are also listed in the table. Crosses indicate the terms that would vanish for  $J_{AC} = 0$  Hz (*i.e.* a linear spin system).

Fig. 2 presents schematic DQ–SQ refocused INADEQUATE spectra of a linear (Fig. 2(a)) and a triangular (Fig. 2(b))  $A$ – $B$ – $C$  spin system. In Fig. 2(b),  $J_{AC}$  corresponds to the long-range (*e.g.* two-bond  $^{13}\text{C}$ – $^{13}\text{C}$ ) coupling, and is such that  $J_{AC} \ll J_{AB}$  and  $J_{AC} \ll J_{BC}$ . The positions of the associated long-range correlations are indicated as filled black squares. The cross peaks arising from direct one-bond connectivities are shown as filled black circles. The position corresponding to the negative relayed peak observed in Fig. 1(b), at the DQ frequency  $\Omega_{AC} = \omega_A + \omega_C$ , and at  $\omega_B$  in the direct dimension, is shown as a crossed circle in Fig. 2(a). In the triangular spin system, two addi-

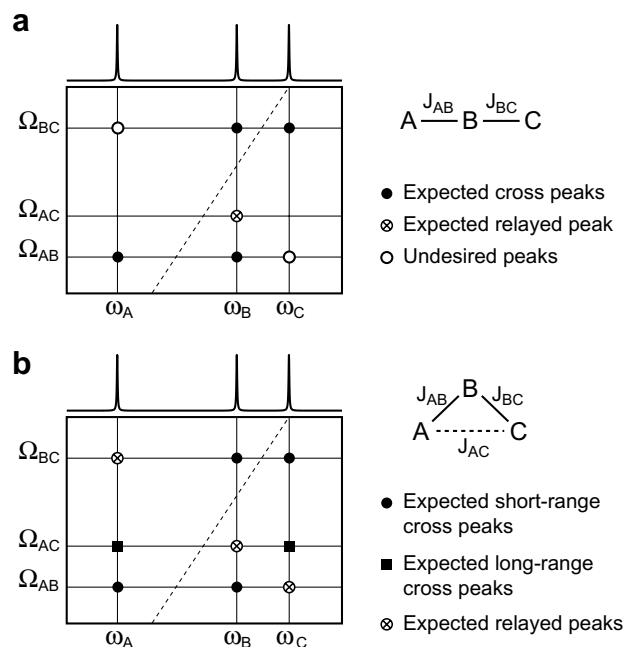


Fig. 2. Schematic INADEQUATE spectra of (a) a linear three-spin system, and (b) a triangular spin system with  $J_{AC}$  corresponding to a two-bond long-range coupling. The expected direct one-bond cross peak positions are indicated as filled black circles and the negative so-called relayed peaks are shown as crossed circles. In (a), the potential positions of undesired peaks that may be observed using the refocused INADEQUATE spectrum in multispin systems are indicated as open circles. In (b) black squares indicate the expected position of the long-range  $A$ – $C$  correlation due to  $J_{AC}$ .

tional low-intensity relayed peaks are expected at  $(\Omega_{AB}, \omega_C)$  and  $(\Omega_{BC}, \omega_A)$ , as shown by the crossed circles in Fig. 2(b). It is clear from Table 1 that only a limited set of terms are responsible for the desired in-phase contributions to the spectrum, namely the  $A_y$ ,  $B_y$  and  $C_y$  coherences, whose positions correspond to the filled and crossed circles in Fig. 2, while all other terms correspond to anti-phase contributions that are spread to different possible positions in the spectrum (including the position of the expected peaks) and should ideally be eliminated.

It is important to note that the amplitudes of these in-phase and anti-phase terms are in principle comparable, so they can make significant contributions to the spectrum. However, it is known from solution-state NMR that the anti-phase terms will be strongly attenuated with increasing linewidth, and thus one may conclude that in solids the contribution is minor. Indeed, in some cases they will not cause an observable effect. This effect is only noticeable in systems with effective correlation linewidths [29,30] (*i.e.* inhomogeneously broadened 1D NMR peaks may in favorable cases yield elongated correlation peaks of remarkably narrow cross section in 2D NMR spectra) comparable to or smaller than the  $J$ -couplings. In reality, with modern decoupling techniques, this is the case in most solids, whether they are small molecule ordered crystals, proteins, or even many disordered solids [29,30,40]. The lineshape distortions discussed here are thus likely to be encountered in most solid-state correlation spectra.

One of our principal aims is to determine whether undesired peaks can appear at the position of long-range correlations  $(\Omega_{AC}, \omega_A)$  and  $(\Omega_{AC}, \omega_C)$  when  $J_{AC} = 0$  Hz, and lead to erroneous interpretation. No such terms can be seen in Table 1. However, they might potentially arise from the other parts of the initial density matrix, namely  $\sigma_0^B = -M_B^0 B_y$  and  $\sigma_0^C = -M_C^0 C_y$ . The cyclic permutation  $A \rightarrow B \rightarrow C \rightarrow A$  applied to the terms at  $(\Omega_{BC}, \omega_B)$  and  $(\Omega_{BC}, \omega_C)$  in Table 1 would give a contribution from  $\sigma_0^B$  to  $A$ - $C$  correlations, but, again, there are no such terms in Table 1. Finally, the contributions from  $\sigma_0^C$  to  $A$ - $C$  correlations are obtained by applying the cyclic permutation  $A \rightarrow C \rightarrow B \rightarrow A$  to the terms at  $(\Omega_{AB}, \omega_A)$  and  $(\Omega_{AB}, \omega_B)$ . These are as follows:

$$\begin{aligned} & \frac{C_y M_C^0}{2} s_{AC}^2 c_{BC}^2 + \frac{2C_x A_z M_C^0}{2} s_{AC} c_{AC} c_{BC}^2 \\ & - \frac{2B_z C_x M_C^0}{2} s_{AC}^2 s_{BC} c_{BC} + \frac{4A_z B_z C_y M_C^0}{2} c_{AC} s_{AC} c_{BC} s_{BC} \end{aligned} \quad (8)$$

for the contribution from  $\sigma_0^C$  at  $(\Omega_{AC}, \omega_C)$ , and:

$$\begin{aligned} & \frac{A_y M_C^0}{2} c_{AB} s_{AC}^2 c_{BC} + \frac{2A_x C_z M_C^0}{2} c_{AB} s_{AC} c_{AC} c_{BC} \\ & - \frac{2A_x B_z M_C^0}{2} s_{AB} s_{AC}^2 c_{BC} + \frac{4A_y B_z C_z M_C^0}{2} s_{AB} c_{AC} s_{AC} c_{BC} \end{aligned} \quad (9)$$

for the contribution from  $\sigma_0^C$  at  $(\Omega_{AC}, \omega_A)$ . All of these terms contain  $s_{AC} = \sin(2\pi J_{AC}\tau)$  or  $s_{AC}^2 = \sin^2(2\pi J_{AC}\tau)$ , and thus vanish for  $J_{AC} = 0$  Hz, which means that, for

$t_1 = 0$ , no other contribution than those due to the  $J_{AC}$  coupling can appear at the expected positions of the long-range  $A$ - $C$  correlations (black squares in Fig. 2(b)). Similarly, it can be shown that the DQ evolution period  $t_1$  would not result in the creation of additional anti-phase peaks at  $(\Omega_{AC}, \omega_A)$  and  $(\Omega_{AC}, \omega_C)$  for  $J_{AC} = 0$  Hz. Thus, even if anti-phase contributions are not removed, the refocused INADEQUATE should provide unambiguous identification of long-range (*e.g.* two-bond  $^{13}\text{C}$ - $^{13}\text{C}$ ) correlations.

The small peaks observed in Fig. 1(c) at  $(\Omega_{AC}, \omega_A)$  and  $(\Omega_{AC}, \omega_C)$  are thus likely due to a non-negligible  $J_{AC}$  coupling. A 1D spectrum (not shown) of uniformly  $^{13}\text{C}$ -enriched L-alanine in solution was recorded which showed a  $^2J(^{13}\text{CO}-^{13}\text{CH}_3)$  coupling of  $1.3 \pm 0.1$  Hz. Although this value is small (compared to  $\sim 35$  Hz for  $^1J(^{13}\text{CH}-^{13}\text{CH}_3)$ ), a  $J_{AC}$  coupling in the solid-state on the order of 2 Hz can potentially lead to long-range peaks of the order of 1% of the intensity of the one-bond direct correlations, as observed here.

Table 2 then shows the complete build-up functions for the desired in-phase terms in a triangular spin system ( $J_{AC} \neq 0$  Hz), obtained for  $t_1 = 0$ , by considering the complete initial density matrix  $\sigma_0 = -M_A^0 A_y - M_B^0 B_y - M_C^0 C_y$ , with  $M_A^0$ ,  $M_B^0$ , and  $M_C^0$  being potentially different, as they depend on the CP efficiency in solids. This corresponds to the build-up functions expected in ideal conditions of complete removal of the undesired anti-phase contributions. The contributions corresponding to the positions indicated by black circles and squares in Fig. 2(b) are clearly identified, as well as the negative relayed peaks at  $(\Omega_{AC}, \omega_B)$ ,  $(\Omega_{AB}, \omega_C)$  and  $(\Omega_{BC}, \omega_A)$ .

Table 2

Refocused INADEQUATE build-up of a triangular spin system ( $J_{AC} \neq 0$  Hz) as a function of  $\tau$ , for  $t_1 = 0$ , in the ideal case of all anti-phase dispersive contributions being removed

Position in the 2D spectrum	Build-up function	Nature
$(\Omega_{AB}, \omega_A)$	$(M_A^0/2)s_{AB}^2 c_{AC}^2 + (M_B^0/2)s_{AB}^2 c_{AC} c_{BC}$	$A$ - $B$ correlation
$(\Omega_{AB}, \omega_B)$	$(M_A^0/2)s_{AB}^2 c_{AC} c_{BC} + (M_B^0/2)s_{AB}^2 c_{BC}^2$	$A$ - $B$ correlation
$(\Omega_{AB}, \omega_C)$	$-(M_C^0/2)s_{AC}^2 s_{BC}^2$	$A$ - $B$ through $C$
$(\Omega_{AC}, \omega_A)$	$(M_A^0/2)c_{AB}^2 s_{AC}^2 + (M_C^0/2)c_{AB} s_{AC}^2 c_{BC}$	$A$ - $C$ correlation
$(\Omega_{AC}, \omega_B)$	$-(M_B^0/2)s_{AB}^2 s_{BC}^2$	$A$ - $C$ through $B$
$(\Omega_{AC}, \omega_C)$	$(M_A^0/2)c_{AB} s_{AC}^2 c_{BC} + (M_C^0/2)s_{AC}^2 c_{BC}^2$	$A$ - $C$ correlation
$(\Omega_{BC}, \omega_A)$	$-(M_A^0/2)s_{AB}^2 s_{AC}^2$	$B$ - $C$ through $A$
$(\Omega_{BC}, \omega_B)$	$(M_B^0/2)c_{AB}^2 s_{BC}^2 + (M_C^0/2)c_{AB} c_{AC} s_{BC}^2$	$B$ - $C$ correlation
$(\Omega_{BC}, \omega_C)$	$(M_B^0/2)c_{AB} c_{AC} s_{BC}^2 + (M_C^0/2)c_{AC}^2 s_{BC}^2$	$B$ - $C$ correlation

$s_{KL}$  and  $c_{KL}$  are, respectively, equal to  $\sin(2\pi J_{KL}\tau)$  and  $\cos(2\pi J_{KL}\tau)$ .  $M_A^0$ ,  $M_B^0$ , and  $M_C^0$  represent the initial magnetization (after CP) on  $A$ ,  $B$ , and  $C$ , respectively.

In conclusion we find that additional terms in three-spin systems lead to lineshape distortions and relayed peaks. They do not lead to the appearance of peaks between uncoupled spins. In the following, several techniques are proposed that provide at least partial removal of the undesired anti-phase and dispersive contributions to the refocused INADEQUATE spectrum, thus tending towards the ideal case whose behavior is summarized in Table 2.

### 3. $z$ -filters and zero-quantum contributions

In solution-state NMR, a  $z$ -filter is commonly employed to improve phase-distorted lineshapes [41]. In the solid-state, Mueller and co-workers have presented UC2QF-COSY [13] and constant-time UC2QF-COSY [14] spectra employing a  $z$ -filter, while  $z$ -filtered refocused INADEQUATE spectra have also been recently presented [22,31,42]. This section shows that an appropriate  $z$ -filter leads to reduction, but not complete removal, of anti-phase contributions to the lineshapes in multispin systems.

To observe only purely in-phase lineshapes, it is necessary to remove the anti-phase terms (compare Tables 1 and 2), while retaining the desired  $A_y$ ,  $B_y$  and  $C_y$  coherences. Consider the effect of a  $90^\circ$  pulse around the  $x$ -axis: this would flip the latter terms onto the  $z$ -axis while converting the anti-phase contributions to a mixture of DQ and zero-quantum (ZQ) terms such as, for example:

$$2A_xB_z \xrightarrow{90_x} -2A_xB_y = (1/2i)(A^-B^- - A^+B^+ + A^+B^- - A^-B^+) \quad (10)$$

and

$$4A_yB_zC_z \xrightarrow{90_x} 4A_zB_yC_y = -A_z(B^+C^+ + B^-C^- - B^+C^- - B^-C^+) \quad (11)$$

Fig. 3 shows the pulse sequence and coherence-transfer pathway diagram for a  $z$ -filtered refocused (zfr-) INADEQUATE experiment. Phase cycling is required to ensure the desired selection of coherence order zero (corresponding also to population states, e.g.  $A_z$ ) between the two

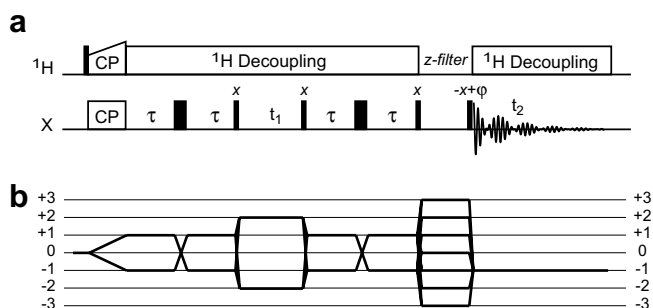


Fig. 3. (a)  $z$ -filtered refocused (zfr) INADEQUATE pulse sequence. (b) Coherence-transfer pathway diagram associated with a zfr-INADEQUATE experiment in a three-spin system. Without phase cycling of the final  $90^\circ$  pulse ( $\phi = 0^\circ$  in the pulse sequence of (a)), all possible coherence pathways are allowed, and undesired contributions are consequently not eliminated.

$90^\circ$  pulses of the  $z$ -filter. Specifically, and as suggested in particular in Refs. [43] and [44] for liquid-state NMR INADEQUATE and refocused INADEQUATE experiments, four-step phase-cycling of the final  $90^\circ$  pulse (consisting of  $\phi = 0, 90, 180, 270^\circ$  and  $\phi_{\text{receiver}} = 0, 90, 180, 270^\circ$ ) is required to remove contributions of coherence order  $\pm 2$ , and thus eliminates half the intensity of the undesired contributions listed in Table 1, which, as described in Eqs. (10) and (11), are converted to a mixture of DQ and ZQ coherences by the first  $90^\circ$  pulse of the  $z$ -filter. It was verified experimentally on fully  $^{13}\text{C}$ -enriched L-alanine (data not shown), that a two-step phase cycle consisting of  $\phi = 0, 180^\circ$  and  $\phi_{\text{receiver}} = 0, 0^\circ$  for a  $z$ -filter of zero duration had no effect on the spectrum, since such a phase cycle also allows DQ coherences to pass through.

Fig. 4(a) shows extracted traces from the zfr-INADEQUATE spectrum of 99%  $^{13}\text{C}$ -enriched L-alanine, with a four-step phase-cycled  $z$ -filter of null duration, otherwise recorded under identical conditions as the one in Fig. 1(b). The comparison between the traces in Fig. 4(a) and in Fig. 1(c) shows a clear reduction but not complete removal of the anti-phase contributions to the intense correlation peaks, namely those corresponding to the directly bonded pairs (solid circles in Fig. 2(a)), and the remote peak (crossed circle in Fig. 2(a)).

Additionally, peaks at other positions of the spectrum show anti-phase peaks of higher intensity than in Fig. 1(c). This is presumably due to the removal of some contributions that cancel out with others in Fig. 1(c). In any case, these peaks remain small. Most importantly, this shows that a four-step-cycled  $z$ -filter of zero duration alone is not sufficient to completely remove the undesired contributions. Indeed, it is known from the discussion above that the four-step phase-cycling removes the DQ coherences, but not the ZQ coherences, which are thus converted back into dispersive anti-phase coherences of the form  $A_xB_z$ ,  $B_zC_x$ ,... Within the framework of the product-operator analysis, the ZQ coherences are therefore the only remaining contribution that must be eliminated during the  $z$ -filter.

Numerical simulations of the  $z$ -filtered refocused INADEQUATE experiment have been carried out using the SIMPSON program [45] on a system including all the anisotropic interactions in order to confirm the nature of the undesired contributions to the experimental spectra, and to validate the above analysis based on product-operator formalism. A linear three-spin system was considered, whose parameters reproduce the intra-molecular carbon spin system of L-alanine, the  $^2J(^{13}\text{CO}-^{13}\text{CH}_3)$  coupling being set to 0 Hz, (see Section 6 for further details). The  $^{13}\text{C}$  Larmor frequency was set to 125.72 MHz (corresponding to a static magnetic field of 11.74 T), with the MAS frequency set equal to 25 kHz to match the experimental conditions. In the following,  $A$ ,  $B$ , and  $C$ , respectively, designate the  $^{13}\text{CO}$ ,  $^{13}\text{CH}$ , and  $^{13}\text{CH}_3$  carbon spins of L-alanine in the simulation.

Fig. 5(a), shows the 1D build-up of the spin  $B$  ( $^{13}\text{CH}$ ) resonance as a function of the  $\tau$  spin-echo delay, for a

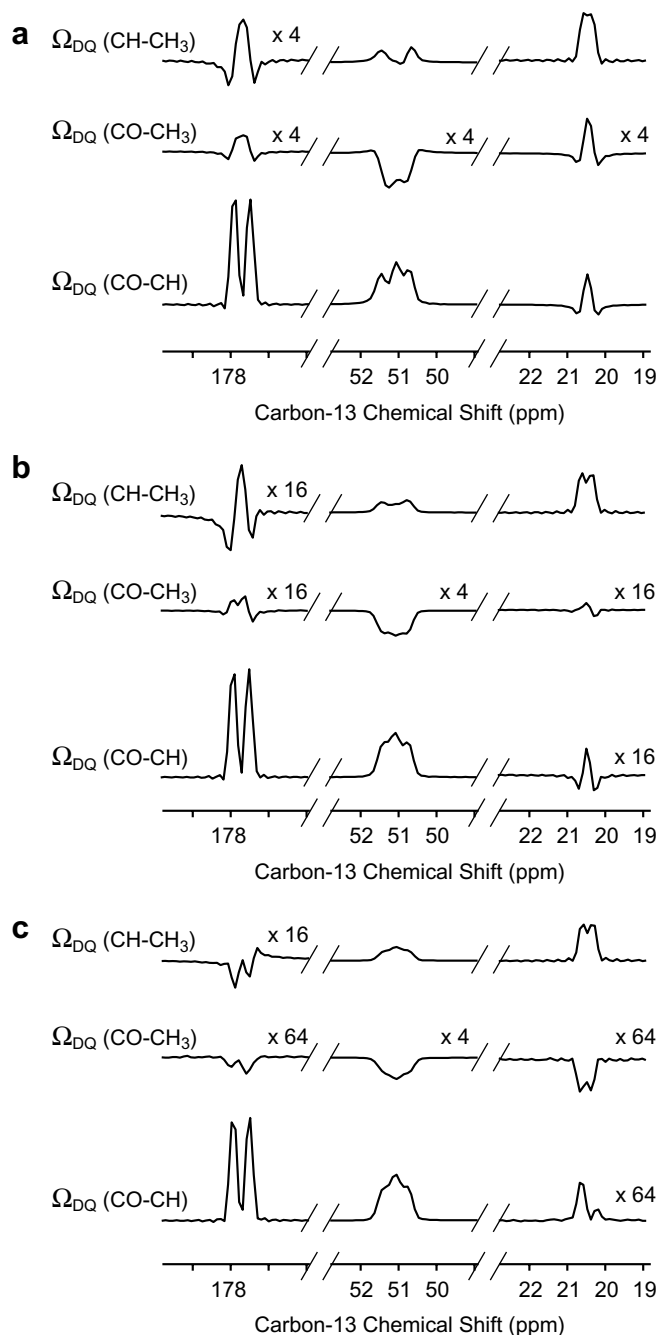


Fig. 4. Series of traces extracted from  $^{13}\text{C}$  zfr-INADEQUATE 2D spectra (not shown) recorded on fully  $^{13}\text{C}$ -enriched L-alanine, using the pulse sequence of Fig. 3(a), with a four-step phase-cycled  $z$ -filter (phase cycling used for the 90 pulse before the  $z$ -filter and the receiver, in degrees, were  $\phi = 0, 90, 180,$  and  $270^\circ$  and  $\phi_{\text{receiver}} = 0, 90, 180,$  and  $270^\circ$ , respectively) of duration (a)  $\tau_z = 0$  ms, (b)  $\tau_z = 1$  ms, and (c)  $\tau_z = 5$  ms. The rows, from top to bottom, respectively, correspond to the double-quantum frequency of the CH-CH<sub>3</sub>, CO-CH<sub>3</sub> and CO-CH correlations, while the columns correspond to the CO, CH and CH<sub>3</sub> in  $F_2$ , respectively. The vertical scaling factor, if any, applied to a given sub-spectrum is indicated on the figure. Experimental conditions were kept identical as for Figs. 1(b and c) to allow direct comparison.

$z$ -filter of null  $\tau_z$  duration during which only density-matrix elements corresponding to coherence order 0 are selected, which corresponds to the experimental case of a

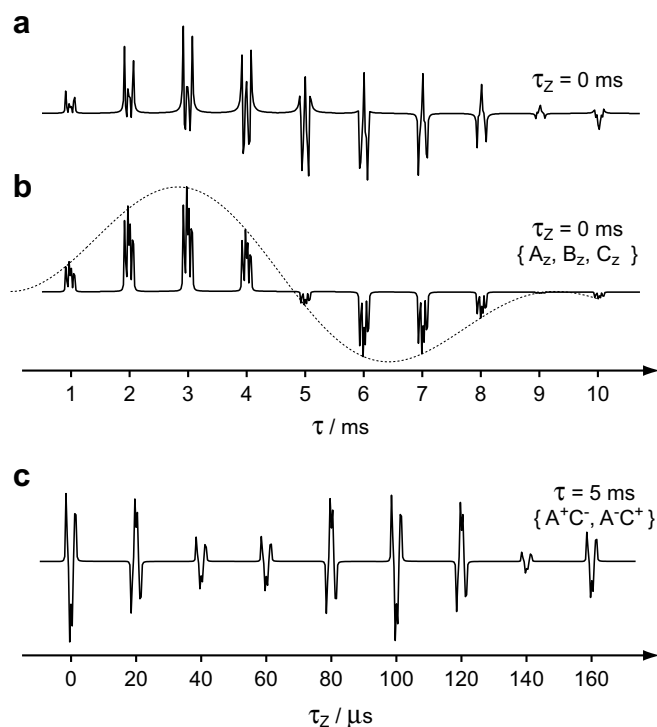


Fig. 5. Numerical (SIMPSON) simulations of the 1D- $z$ -filtered-INADEQUATE experiment applied to a the  $^{13}\text{C}$  three-spin linear system corresponding to L-alanine (see Ref. [58]).  $A$ ,  $B$ , and  $C$ , respectively, designate the CO, CH and CH<sub>3</sub> signals of L-alanine. The  $^{13}\text{C}$  Larmor frequency was set to 125.72 MHz, and a spinning frequency of 25 kHz was used. Only the peak corresponding to spin  $B$  is shown here, as a function of the half-spin-echo duration  $\tau$  (a and b) or the  $z$ -filter duration  $\tau_z$  (c). (a) Density-matrix elements corresponding to coherence order 0 are selected, thus leading to the experimental case of a four-step phase-cycled  $z$ -filter where both population states and ZQ coherences pass through. (b) Only populations are selected during the  $z$ -filter ( $A_z, B_z, C_z$ ). The dotted line shows the best fit obtained with the expected build-up of the ( $\Omega_{AB}, \omega_B$ ), ( $\Omega_{AC}, \omega_B$ ) and ( $\Omega_{BC}, \omega_B$ ) terms in Table 2, yielding  $J_{AB}$  and  $J_{BC}$  coupling values of 34.0 and 53.9 Hz, respectively, compared to 34.0 and 54.0 Hz used for the numerical simulation. (c) Only  $A^+C^-$  and  $A^-C^+$  ZQ coherences have been selected during the  $z$ -filter. Pure anti-phase dispersive signal is observed in this case. The evolution as a function of the  $z$ -filter duration  $\tau_z$  corresponds to a modulation at the frequency  $|\omega_A - \omega_C|$ .

four-step phase-cycled  $z$ -filter where both population states and ZQ coherences pass through. Anti-phase contributions are clearly visible, illustrating the incomplete removal of the undesired terms. For comparison, Fig. 5(b) presents the results of identical simulations, except that only density-matrix elements corresponding to populations ( $A_z, B_z,$  or  $C_z$  terms) are allowed during the  $z$ -filter. The pure in-phase absorptive shape of the resulting lines shows that the undesired anti-phase components arise exclusively from the ZQ order terms of the form  $A^+B^-$  (and  $A^+B^-C_z$ ) during the  $z$ -filter. It should be noted that the build-up is a sum of the evolution as a function of  $\tau$  for three distinct peaks in the 2D spectrum, namely peaks at  $\Omega_{AB}$ ,  $\Omega_{BC}$ , and  $\Omega_{AC}$  in the indirect dimension, and  $\omega_B$  in the direct dimension. The best fit shown as a dotted line in Fig. 5(b), using the appropriate build-up curves of Table 2 with

$M_A^0 = M_B^0 = M_C^0$  and  $J_{AC} = 0$  Hz, yields fitted  $J_{AB}$  and  $J_{BC}$  coupling values in excellent agreement (within 0.2%) with the 34.0 and 54.0 Hz values used for the simulation, which validates the solution-state product-operator analysis presented above.

In Fig. 5(c), where only coherences  $A^+C^-$  and  $A^-C^+$  have been selected, for  $\tau = 5$  ms, we observe pure anti-phase lineshapes whatever the length of the  $z$ -filter  $\tau_Z$  is, and the same is true for other types of ZQ term ( $A^+B^-$ ,  $A^-B^+$ ,  $B^+C^-$ , or  $B^-C^+$ ) being selected during the  $z$ -filter (data not shown). This proves that all the desired contributions have the form of populations during the  $z$ -filter, as expected from the product-operator analysis, and additionally confirms that the issue to be tackled here is the suppression of ZQ contributions. This is furthermore supported in Fig. 5(c) by the evolution as a function of  $\tau_Z$  of the signal of spin  $B$ , which shows the expected modulation at the frequency difference  $|\omega_A - \omega_C|$  between  $A$  and  $C$  resonances (*ca.* 19.7 kHz at 11.74 T).

#### 4. Removing zero-quantum coherences

First, it should be noted that the removal of such undesired contributions from 2D NMR spectra is not a recent issue. In a key paper published in 1981, Macura et al. [46] have shown that undesired  $J$  cross-peaks observed in 2D exchange and/or NOE spectra in solution were arising from single, double and zero-quantum coherences created before the mixing time through  $J$ -coupling evolution. First, they proposed to remove single and double-quantum coherences by phase cycling (or by using pulsed field gradients). As illustrated in the previous subsection, this turns out also to work well in powdered solids under fast MAS conditions. Second, since ZQ coherences are insensitive to phase shifts as well as to magnetic field inhomogeneity, several approaches were proposed to remove them, which are reviewed below, together with alternative methods that have been proposed more recently.

As mentioned above, the use of efficient decoupling techniques and fast MAS in high-resolution spin-1/2 NMR of powdered crystalline solids provides narrow lines, in which anti-phase contributions can be problematic. Even in disordered solids, it has been shown that narrow lines could be observed in 2D refocused INADEQUATE spectra in some cases [29] suggesting that recording purely in-phase spectra may also become an issue in that case. Under such conditions, we expect ZQ coherences to have a near-solution-state behavior, and the application of methods to remove ZQ coherences in solution is therefore briefly reviewed.

The first method to remove ZQ coherences in solution, proposed by Macura et al. [46] consists of the use of random variations of the  $z$ -filter length (or mixing time in the context of Ref. [46]), during which ZQ coherences evolve while  $z$ -magnetization is kept unchanged. If the overall duration sampled by these variable delays is longer than half of the longest period of the ZQ coherences (*i.e.* the inverse of the smallest chemical shift difference between

two spins of a given spin system; *i.e.*  $\pi/|\omega(\text{CH}) - \omega(\text{CH}_3)|$  in L-alanine), the summation of a sufficiently large number of experiments will result in the cancellation of the undesired terms by destructive interference. This method has the disadvantage of requiring a dramatic increase of the experimental time. However, this can be avoided by randomly varying the  $z$ -filter duration and simultaneously incrementing  $t_1$ , which however results in so-called  $t_1$  noise in the indirect dimension [46]. The second method proposed in Ref. [46] introduces a  $180^\circ$  pulse inside the  $z$ -filter whose position changes from one experiment to another. This results in a variable evolution period of the ZQ coherences (since a variable part of their evolution is refocused), while keeping the overall duration of the filter constant, population states being not affected (only inverted) by the  $180^\circ$  pulse. This method is of particular interest in cases where the filter period is used as a mixing time, whose overall duration should remain constant. Several variants of this method have since been introduced, such as an optimized set of evolution delays instead of random durations [47] and recently, a novel variant was proposed in which the desired cancellation can be obtained in a single transient [48]. By means of a field gradient, the Larmor frequencies are made space-dependent, and a swept-frequency  $180^\circ$  pulse therefore refocuses the spins at different positions in the sample at different times. Finally, other methods were proposed, some of which are quite efficient and easy to implement, such that their application to obtain pure in-phase absorptive spectra in multispin solids under MAS could be envisaged [49–54].

In solid-state NMR, alternative approaches can be proposed to overcome the problem of ZQ coherences that generate undesired anti-phase contributions to the refocused INADEQUATE spectra of multispin systems. In particular, we shall discuss here the effects of the residual heteronuclear couplings that are not completely averaged out by MAS in the absence of heteronuclear decoupling. These heteronuclear dipolar couplings are presumed to have a large contribution to the ZQ-lineshape in solids under MAS, thus leading to dephasing of ZQ coherences. As a consequence, the introduction of strong heteronuclear couplings by switching off the heteronuclear decoupling during the  $z$ -filter is likely to be an efficient way to induce fast dephasing of the undesired contributions.

However, a potential drawback of this method is that proton-driven spin-diffusion [55] (PDS) between carbons that are close in space may then also occur during the  $z$ -filter, since this also depends on the size of the effective heteronuclear dipolar-coupling constant.

We have recently shown that in weakly proton-coupled systems such as partially  $^{29}\text{Si}$ -enriched surfactant-templated layered silicates,  $z$ -filters as long as 50 ms could safely be used at 10 kHz MAS since no  $^{29}\text{Si}$ – $^{29}\text{Si}$  PDS occurs in this period [56]. Another favorable example has been demonstrated in Ref. [57], where  $z$ -filters of 10 ms have been used during which we showed that no  $^{31}\text{P}$ – $^{31}\text{P}$  proton-driven spin-diffusion occurred at high spinning

frequencies. This enabled the recording of  $^{31}\text{P}$  INADEQUATE-based 2D spectra free of anti-phase contributions (in a two-spin system in this case). In such cases, long  $z$ -filters without heteronuclear decoupling offer a fully satisfactory solution, which in addition reduces the probe duty cycle, as has been exploited in Ref. [56]. This can be of crucial importance when measuring long-range correlations through weak scalar couplings.

Nevertheless, the situation is not as favorable in (generally) strongly-coupled organic systems, where PDSO occurs much more rapidly. In this case a compromise must be found between the  $z$ -filter duration, and spin diffusion rates. We show in Fig. 4(b and c) two series of traces extracted from two zfr-INADEQUATE spectra recorded under the same conditions as in Fig. 4(a), except that  $z$ -filter durations of 1 ms (Fig. 4(b)) and 5 ms (Fig. 4(c)) without heteronuclear decoupling were used. The improvement in terms of lineshapes is clear between  $\tau_z = 0$  and 1 ms (Fig. 4(a) and 4(b)) and then 5 ms (Fig. 4(c)). In particular, peaks at  $(\Omega_{\text{DQ}}(\text{CH}-\text{CH}_3), \omega(\text{CH}))$  and  $(\Omega_{\text{DQ}}(\text{CO}-\text{CH}), \omega(\text{CH}))$ , which appeared somewhat distorted for  $\tau_z = 0$  ms (Fig. 4(a)), show increased sensitivity and better lineshapes in Fig. 4(b) for  $\tau_z = 1$  ms. Even better lineshapes are observed for  $\tau_z = 5$  ms (Fig. 4(c)), where the multiplet structure expected for the CH peak of polycrystalline L-alanine under such conditions [58] can be identified at  $(\Omega_{\text{DQ}}(\text{CH}-\text{CH}_3), \omega(\text{CH}))$  and  $(\Omega_{\text{DQ}}(\text{CO}-\text{CH}), \omega(\text{CH}))$ . The four peaks that do not correspond to direct one-bond correlations or to the CO-CH<sub>3</sub> relayed peak, namely peaks at  $(\Omega_{\text{DQ}}(\text{CO}-\text{CH}), \omega(\text{CH}_3))$ ,  $(\Omega_{\text{DQ}}(\text{CO}-\text{CH}_3), \omega(\text{CO}))$ ,  $(\Omega_{\text{DQ}}(\text{CO}-\text{CH}_3), \omega(\text{CH}_3))$  and  $(\Omega_{\text{DQ}}(\text{CH}-\text{CH}_3), \omega(\text{CO}))$ , also show nearly pure in-phase lineshapes for a 5 ms  $z$ -filter (Fig. 4(c)), indicating an almost complete removal of the undesired contributions. For  $J_{AC} \neq 0$ , peaks at  $(\Omega_{AB}, \omega_C)$  and  $(\Omega_{BC}, \omega_A)$  (i.e.  $(\Omega_{\text{DQ}}(\text{CO}-\text{CH}), \omega(\text{CH}_3))$  and  $(\Omega_{\text{DQ}}(\text{CH}-\text{CH}_3), \omega(\text{CO}))$  for L-alanine) correspond to the expected position of the A-B and B-C relayed cross peaks, respectively, as indicated by the crossed circles in Fig. 2(b). Thus, the in-phase signal expected at these positions should be negative, which is obviously not the case at  $(\Omega_{\text{DQ}}(\text{CO}-\text{CH}), \omega(\text{CH}_3))$ , where a (very small though) in-phase positive peak can be seen. This peak thus probably arises from magnetization transfer from  $B_z$  to  $C_z$  during the  $z$ -filter due to proton-driven spin diffusion.

Although contributions from spin diffusion are clearly weak for  $\tau_z = 5$  ms, and do not perturb short range correlations, they may be problematic when long-range correlations are expected. Indeed, the negative peaks observed in Fig. 4(c) at  $(\Omega_{\text{DQ}}(\text{CO}-\text{CH}_3), \omega(\text{CO}))$  and  $(\Omega_{\text{DQ}}(\text{CO}-\text{CH}_3), \omega(\text{CH}_3))$  also probably arise from proton-driven spin diffusion from  $B_z$  (negative at  $\Omega_{AC}$ ) to  $A_z$  and to  $C_z$ , and interfere with the observation of small long-range cross peaks due to  $J_{AC}$  (see Table 2). As a result, in such cases, the implementation of some of the solution-state-based approaches discussed above in this section might be more appropriate, and hopefully allow the measurement of unambiguous pure phase refocused INADEQUATE spectra

showing long-range correlations in solid-state NMR of isotopically labeled bio-macromolecules.

## 5. Conclusions

A detailed investigation of the widely-used refocused INADEQUATE pulse sequence has been presented for the case of a fully isotopically enriched three-spin system. The approach is based on a solution-state product-operator analysis, which proves to be suitable for solids under fast MAS for the case of  $^{13}\text{C}$ -labeled L-alanine. We describe in detail the origin of multispin contributions to the refocused INADEQUATE spectra, which can seriously affect the appearance of lineshapes for the direct one-bond correlations, and lead to additional anti-phase and “relayed” peaks. However, we show that undesired multispin contributions do not in any case interfere with the observation of long-range correlations. Properly cycled  $z$ -filters are shown to partially eliminate these contributions. The remaining contributions are identified as zero-quantum coherences, for which solutions achieving their elimination have been proposed in solution-state NMR over the last two decades. We discuss a simple solid-state approach based on the dephasing of zero-quantum coherences by residual heteronuclear couplings in the absence of heteronuclear decoupling, which can be fully satisfactory in weakly proton-coupled systems.

Finally, we note that the considerations here are also applicable to zero-quantum lineshape artifacts that may appear in homonuclear ( $^{13}\text{C}$ ) PDSO experiments widely used currently in protein NMR studies [59–62]. Thus, zero-quantum lineshapes distortions will be absent at longer mixing times due to the dephasing mechanism considered above, but they should be present for short (or zero) mixing times (and could notably affect calibration spectra for quantitative determinations).

## 6. Experimental and simulation details

### 6.1. NMR measurements

All the spectra reported in this paper were recorded on a Bruker AVANCE spectrometer operating at  $^1\text{H}$  and  $^{13}\text{C}$  Larmor frequencies of 500.13 and 125.76 MHz, respectively. The 2D refocused and zfr-INADEQUATE spectra were obtained using a 2.5 mm MAS double resonance ( $^{13}\text{C}-^1\text{H}$ ) probe at a spinning frequency of 25 kHz. The proton  $90^\circ$  pulse was 2.5  $\mu\text{s}$ . Ramped cross-polarization [63] using a contact time of 1.676 ms was used to transfer the magnetization from protons to carbons. SPINAL-64 proton decoupling [64] was applied during evolution and acquisition periods at a RF field of 140 kHz. Carbon  $90^\circ$  and  $180^\circ$  pulse lengths of 3.5 and 7  $\mu\text{s}$ , respectively, were used. Unless otherwise stated, the  $\tau$  delay was set to 3 ms. Quadrature detection in  $t_1$  was achieved using the TPPI method [65] with 32 transients being co-added for each of the 500  $t_1$  increments. The total acquisition time

in  $t_1$  and  $t_2$  were 10 and 30 ms, respectively. The recycle delay was 2.5 s.

## 6.2. Numerical simulations

All simulation results were obtained using the SIMPSON simulation program [45], based on standard numerical techniques [66], for a three-spin system whose parameters correspond to the intra-molecular  $^{13}\text{C}$  spin system of fully labeled L-alanine, and were chosen as in Ref. [58]. The powder average was performed using a set of 143  $\{\alpha, \beta\}$  angles generated by the ZCW algorithm [67] and 10 evenly spaced values of the third Euler angle  $\gamma$ . No significant changes in the lineshapes were observed upon further increase of the number of orientations. The static magnetic field was set to 11.74 T ( $^1\text{H}$  Larmor frequency of 500.0 MHz), and a MAS frequency of 25 kHz was used. Hard pulses were taken to be ‘ideal’ pulses (*i.e.*, no evolution occurs during the pulse). The  $\tau$  delays and the  $z$ -filter durations  $\tau_z$  were chosen to be multiples of a rotor period. Transverse dephasing was artificially inserted during the processing by using 10-Hz Lorentzian line broadening. The SIMPSON input files used for the numerical simulations are available upon request to the authors.

## Acknowledgments

Some of the authors (S.C., L.E., T.N.P., and S.P.B.) are grateful to EGIDE/British Council funding of an Alliance Franco-British international exchange Grant. S.P.B. and T.N.P. thank EPSRC for funding. J.H.B. acknowledges the Fulbright Scholars program for support.

## References

- [1] M. Baldus, B.H. Meier, Total correlation spectroscopy in the solid state. The use of scalar couplings to determine the through-bond connectivity, *J. Magn. Reson. Ser. A* 121 (1996) 65–69.
- [2] M. Baldus, R.J. Iulucci, B.H. Meier, Probing through-bond connectivities and through-space distances in solids by magic-angle-spinning nuclear magnetic resonance, *J. Am. Chem. Soc.* 119 (1997) 1121–1124.
- [3] A.S.D. Heindrichs, H. Geen, C. Giordani, J.J. Titman, Improved scalar shift correlation NMR spectroscopy in solids, *Chem. Phys. Lett.* 335 (2001) 89–96.
- [4] J.C.C. Chan, G. Brunklaus, R sequences for the scalar-coupling mediated homonuclear correlation spectroscopy under fast magic-angle spinning, *Chem. Phys. Lett.* 349 (2001) 104–112.
- [5] E.H. Hardy, A. Detken, B.H. Meier, Fast-MAS total through-bond correlation spectroscopy using adiabatic pulses, *J. Magn. Reson.* 165 (2003) 208–218.
- [6] A.A. Maudsley, A. Wokaun, R.R. Ernst, Coherence transfer echoes, *Chem. Phys. Lett.* 55 (1978) 9–14.
- [7] C.A. Fyfe, H. Grondey, Y. Feng, G.T. Kokotailo, Natural-Abundance 2-Dimensional Si-29 MAS NMR investigation of the 3-dimensional bonding connectivities in the zeolite catalyst ZSM-5, *J. Am. Chem. Soc.* 112 (1990) 8812–8820.
- [8] A. Lesage, C. Auger, S. Caldarelli, L. Emsley, Determination of through-bond carbon-carbon connectivities in solid-state NMR using the INADEQUATE experiment, *J. Am. Chem. Soc.* 119 (1997) 7867–7868.
- [9] R. Verel, J.D. van Beek, B.H. Meier, INADEQUATE-CR experiments in the solid state, *J. Magn. Reson.* 140 (1999) 300–303.
- [10] A. Lesage, M. Bardet, L. Emsley, Through-bond carbon-carbon connectivities in disordered solids by NMR, *J. Am. Chem. Soc.* 121 (1999) 10987–10993.
- [11] L.J. Mueller, D.W. Elliott, K.C. Kim, C.A. Reed, P.D.W. Boyd, Establishing through-bond connectivity in solids with NMR: Structure and dynamics in HC60+, *J. Am. Chem. Soc.* 124 (2002) 9360–9361.
- [12] R.A. Olsen, J. Struppe, D.W. Elliott, R.J. Thomas, L.J. Mueller, Through-bond C-13–C-13 correlation at the natural abundance level: Refining dynamic regions in the crystal structure of vitamin-D-3 with solid-state NMR, *J. Am. Chem. Soc.* 125 (2003) 11784–11785.
- [13] L.J. Mueller, D.W. Elliott, G.M. Leskowitz, J. Struppe, R.A. Olsen, K.C. Kim, C.A. Reed, Uniform-sign cross-peak double-quantum-filtered correlation spectroscopy, *J. Magn. Reson.* 168 (2004) 327–335.
- [14] L.L. Chen, R.A. Olsen, D.W. Elliott, J.M. Boettcher, D.H.H. Zhou, C.M. Rienstra, L.J. Mueller, Constant-time through-bond C-13 correlation spectroscopy for assigning protein resonances with solid-state NMR spectroscopy, *J. Am. Chem. Soc.* 128 (2006) 9992–9993.
- [15] F. Fayon, C. Roiland, L. Emsley, D. Massiot, Triple-quantum correlation NMR experiments in solids using J-couplings, *J. Magn. Reson.* 179 (2006) 49–57.
- [16] G. Grasso, T.M. de Swiet, J.J. Titman, Electronic structure of the polymer phase of CsC60: refocused INADEQUATE experiments, *J. Phys. Chem. B* 106 (2002) 8676–8680.
- [17] G. De Paepe, N. Giraud, A. Lesage, P. Hodgkinson, A. Bockmann, L. Emsley, Transverse dephasing optimized solid-state NMR spectroscopy, *J. Am. Chem. Soc.* 125 (2003) 13938–13939.
- [18] H. Kono, Y. Numata, T. Erata, M. Takai, C-13 and H-1 resonance assignment of mercerized cellulose II by two-dimensional MAS NMR spectroscopies, *Macromolecules* 37 (2004) 5310–5316.
- [19] H. Kono, Y. Numata, T. Erata, M. Takai, Structural analysis of cellulose triacetate polymorphs by two-dimensional solid-state C-13–C-13 and H-1–C-13 correlation NMR spectroscopies, *Polymer* 45 (2004) 2843–2852.
- [20] G. Pintacuda, N. Giraud, R. Piratelli, A. Böckmann, I. Bertini, L. Emsley, Solid-state NMR spectroscopy of a paramagnetic protein: assignment and study of human dimeric oxidized CuII–ZnII superoxide dismutase (SOD), *Angew. Chem.-Int. Edit. Engl.* 46 (2007) 1079–1082.
- [21] S.P. Brown, M. Perez-Torralba, D. Sanz, R.M. Claramunt, L. Emsley, The direct detection of a hydrogen bond in the solid state by NMR through the observation of a hydrogen-bond mediated N-15–N-15 J coupling, *J. Am. Chem. Soc.* 124 (2002) 1152–1153.
- [22] T.N. Pham, S. Masiero, G. Gottarello, S.P. Brown, Identification by N-15 refocused inadequate MAS NMR of intermolecular hydrogen bonding that directs the self-assembly of modified DNA bases, *J. Am. Chem. Soc.* 127 (2005) 16018–16019.
- [23] G. De Paepe, A. Lesage, S. Steuernagel, L. Emsley, Transverse dephasing optimised NMR spectroscopy in solids: natural-abundance C-13 correlation spectra, *ChemPhysChem* 5 (2004) 869–875.
- [24] H. Kono, T. Erata, M. Takai, Determination of the through-bond carbon-carbon and carbon-proton connectivities of the native celluloses in the solid state, *Macromolecules* 36 (2003) 5131–5138.
- [25] H. Kono, Two-dimensional magic angle spinning NMR investigation of naturally occurring chitins: precise H-1 and C-13 resonance assignment of alpha- and beta-chitin, *Biopolymers* 75 (2004) 255–263.
- [26] J. Brus, A. Jegorov, Through-bonds and through-space solid-state NMR correlations at natural isotopic abundance: Signal assignment and structural study of simvastatin, *J. Phys. Chem. A* 108 (2004) 3955–3964.
- [27] R.K. Harris, S.A. Joyce, C.J. Pickard, S. Cadars, L. Emsley, Assigning carbon-13 NMR spectra to crystal structures by the

- INADEQUATE pulse sequence and first principles computation: a case study of two forms of testosterone, *Phys. Chem. Chem. Phys.* 8 (2006) 137–143.
- [28] R.K. Harris, S. Cadars, L. Emsley, J.R. Yates, C.J. Pickard, R.K.R. Jetti, U.J. Griesser, NMR crystallography of oxybuprocaine hydrochloride, modification II°, *Phys. Chem. Chem. Phys.* 9 (2007) 360–368.
- [29] D. Sakellariou, S.P. Brown, A. Lesage, S. Hediger, M. Bardet, C.A. Meriles, A. Pines, L. Emsley, High-resolution NMR correlation spectra of disordered solids, *J. Am. Chem. Soc.* 125 (2003) 4376–4380.
- [30] S. Cadars, A. Lesage, L. Emsley, Chemical shift correlations in disordered solids, *J. Am. Chem. Soc.* 127 (2005) 4466–4476.
- [31] J.S.A. Gunne, J. Beck, W. Hoffbauer, P. Krieger-Beck, The structure of poly(carbonsuboxide) on the atomic scale: a solid-state NMR study, *Chem.-Eur. J.* 11 (2005) 4429–4440.
- [32] F. Fayon, G. Le Saout, L. Emsley, D. Massiot, Through-bond phosphorus-phosphorus connectivities in crystalline and disordered phosphates by solid-state NMR, *Chem. Commun.* (2002) 1702–1703.
- [33] F. Fayon, I.J. King, R.K. Harris, R.K.B. Gover, J.S.O. Evans, D. Massiot, Characterization of the room-temperature structure of SnP2O7 by P-31 through-space and through-bond NMR correlation spectroscopy, *Chem. Mat.* 15 (2003) 2234–2239.
- [34] F. Fayon, I.J. King, R.K. Harris, J.S.O. Evans, D. Massiot, Application of the through-bond correlation NMR experiment to the characterization of crystalline and disordered phosphates, *C. R. Chim.* 7 (2004) 351–361.
- [35] F. Fayon, D. Massiot, M.H. Levitt, J.J. Titman, D.H. Gregory, L. Duma, L. Emsley, S.P. Brown, Through-space contributions to two-dimensional double-quantum  $J$  correlation NMR spectra of magic-angle-spinning solids, *J. Chem. Phys.* 122 (2005) 194313–194327.
- [36] D.H. Brouwer, P.E. Kristiansen, C.A. Fyfe, M.H. Levitt, Symmetry-based Si-29 dipolar recoupling magic angle spinning NMR spectroscopy: a new method for investigating three-dimensional structures of zeolite frameworks, *J. Am. Chem. Soc.* 127 (2005) 542–543.
- [37] G. Bodenhausen, H. Kogler, R.R. Ernst, Selection of coherence-transfer pathways in NMR pulse experiments, *J. Magn. Reson.* 58 (1984) 370–388.
- [38] O.W. Sorensen, G.W. Eich, M.H. Levitt, G. Bodenhausen, R.R. Ernst, Product operator-formalism for the description of NMR pulse experiments, *Prog. Nucl. Magn. Reson. Spectrosc.* 16 (1983) 163–192.
- [39] R.R. Ernst, G. Bodenhausen, A. Wokaun, *Principles of Nuclear Magnetic Resonance in One and Two Dimensions*, Oxford Science Publications, New York, 1987.
- [40] N. Hedin, R. Graf, S.C. Christiansen, C. Gervais, R.C. Hayward, J. Eckert, B.F. Chmelka, Structure of a surfactant-templated silicate framework in the absence of 3D crystallinity, *J. Am. Chem. Soc.* 126 (2004) 9425–9432.
- [41] O.W. Sorensen, M. Rance, R.R. Ernst, Z-filters for purging phase-distorted or multiplet-distorted spectra, *J. Magn. Reson.* 56 (1984) 527–534.
- [42] F. Fayon, Personal Communication.
- [43] M. Novic, H. Oschkinat, P. Pfandler, G. Bodenhausen, Z-filtered double-quantum NMR-spectra and automated-analysis by pattern-recognition, *J. Magn. Reson.* 73 (1987) 493–511.
- [44] S. Wimperis, Correlation of connected double-quantum and single-quantum transitions—2-dimensional double-quantum spectroscopy with simplified in-phase direct connectivity multiplets, *J. Magn. Reson.* 87 (1990) 174–182.
- [45] M. Bak, J.T. Rasmussen, N.C. Nielsen, SIMPSON: a general simulation program for solid-state NMR spectroscopy, *J. Magn. Reson.* 147 (2000) 296–330.
- [46] S. Macura, Y. Huang, D. Suter, R.R. Ernst, Two-dimensional chemical-exchange and cross-relaxation spectroscopy of coupled nuclear spins, *J. Magn. Reson.* 43 (1981) 259–281.
- [47] M. Rance, G. Bodenhausen, G. Wagner, K. Wuthrich, R.R. Ernst, A systematic-approach to the suppression of J-cross peaks in 2D exchange and 2D NOE spectroscopy, *J. Magn. Reson.* 62 (1985) 497–510.
- [48] M.J. Thrippleton, J. Keeler, Elimination of zero-quantum interference in two-dimensional NMR spectra, *Angew. Chem.-Int. Edit.* 42 (2003) 3938–3941.
- [49] S. Macura, K. Wuthrich, R.R. Ernst, Separation and suppression of coherent transfer effects in two-dimensional NOE and chemical-exchange spectroscopy, *J. Magn. Reson.* 46 (1982) 269–282.
- [50] J.J. Titman, A.L. Davis, E.D. Laue, J. Keeler, Selection of coherence transfer pathways using inhomogeneous adiabatic pulses—removal of zero-quantum coherence, *J. Magn. Reson.* 89 (1990) 176–183.
- [51] G. Estcourt, A.L. Davis, J. Keeler, Suppression of zero-quantum interference in 2-dimensional Z-COSY spectra, *J. Magn. Reson.* 96 (1992) 191–198.
- [52] A.L. Davis, G. Estcourt, J. Keeler, E.D. Laue, J.J. Titman, Improvement of Z filters and purging pulses by the use of zero-quantum dephasing in inhomogeneous B1 or B0 fields, *J. Magn. Reson. Ser. A* 105 (1993) 167–183.
- [53] K.E. Cano, M.J. Thrippleton, J. Keeler, A.J. Shaka, Cascaded z-filters for efficient single-scan suppression of zero-quantum coherence, *J. Magn. Reson.* 167 (2004) 291–297.
- [54] P.W.A. Howe, Removal of zero-quantum peaks from 1D selective TOCSY and NOESY spectra, *J. Magn. Reson.* 179 (2006) 217–222.
- [55] K. Schmidt-Rohr, H.W. Spiess, *Multi-Dimensional Solid-State NMR and Polymers*, Academic Press, San Diego, 1994.
- [56] S. Cadars, A. Lesage, N. Hedin, B.F. Chmelka, L. Emsley, Selective NMR measurements of homonuclear scalar couplings in isotopically enriched solids, *J. Phys. Chem. B* 110 (2006) 16982–16991.
- [57] S. Cadars, A. Lesage, M. Trierweiler, L. Heux, L. Emsley, NMR measurements of J-coupling distributions in disordered solids, *Phys. Chem. Chem. Phys.* 9 (2007) 92–103.
- [58] L. Duma, S. Hediger, A. Lesage, D. Sakellariou, L. Emsley, Carbon-13 lineshapes in solid-state NMR of labeled compounds. Effects of coherent CSA-dipolar cross-correlation, *J. Magn. Reson.* 162 (2003) 90–101.
- [59] F. Castellani, B. van Rossum, A. Diehl, M. Schubert, K. Rehbein, H. Oschkinat, Structure of a protein determined by solid-state magic-angle-spinning NMR spectroscopy, *Nature* 420 (2002) 98–102.
- [60] A. Bockmann, A. Lange, A. Galinier, S. Luca, N. Giraud, M. Juy, H. Heise, R. Montserret, F. Penin, M. Baldus, Solid state NMR sequential resonance assignments and conformational analysis of the  $2 \times 10.4$  kDa dimeric form of the *Bacillus subtilis* protein Crh, *J. Biomol. NMR* 27 (2003) 323–339.
- [61] A.J. van Gammeren, F. Buda, F.B. Hulsbergen, S. Kiihne, J.G. Hollander, T.A. Egorova-Zachernyuk, N.J. Fraser, R.J. Cogdell, H.J.M. de Groot, Selective chemical shift assignment of B800 and B850 bacteriochlorophylls in uniformly [C-13,N-15]-labeled light-harvesting complexes by solid-state NMR spectroscopy at ultra-high magnetic field, *J. Am. Chem. Soc.* 127 (2005) 3213–3219.
- [62] M. Hiller, L. Krabben, K.R. Vinothkumar, F. Castellani, B.J. van Rossum, W. Kuhlbrandt, H. Oschkinat, Solid-state magic-angle spinning NMR of outer-membrane protein G from *Escherichia coli*, *Chembiochem* 6 (2005) 1679–1684.
- [63] G. Metz, X.L. Wu, S.O. Smith, Ramped-amplitude cross-polarization in magic-angle-spinning NMR, *J. Magn. Reson. Ser. A* 110 (1994) 219–227.
- [64] B.M. Fung, A.K. Khitrin, K. Ermolaev, An improved broadband decoupling sequence for liquid crystals and solids, *J. Magn. Reson.* 142 (2000) 97–101.
- [65] D. Marion, K. Wuthrich, Application of phase sensitive two-dimensional correlated spectroscopy (COSY) for measurements of H-1-H-1 Spin-Spin coupling-constants in proteins, *Biochem. Biophys. Res. Commun.* 113 (1983) 967–974.
- [66] P. Hodgkinson, L. Emsley, Numerical simulation of solid-state NMR experiments, *Prog. Nucl. Magn. Reson. Spectrosc.* 36 (2000) 201–239.
- [67] H. Conroy, *Molecular Schrodinger Equation*. 8. A new method for evaluation of multidimensional integrals, *J. Chem. Phys.* 47 (1967) 5307–5318.